Numerical study on the dynamics of a driven disordered vortex lattice

Yigang Cao, Zhengkuan Jiao, and Heping Ying
Department of Physics, Zhejiang University, Hangzhou 310027, People's Republic of China
(Received 30 November 1999; revised manuscript received 8 March 2000)

Using a model of long-range interactions between vortices, we numerically investigate the dynamics of a driven vortex lattice subject to the randomly distributed pointlike pinning centers in a thin superconducting film. At zero temperature, crossover from elastic to plastic depinnings is observed with increasing density of pinning centers. With the lattice softness, the scaling fit between force and velocity obtained in the elastic regime becomes invalid when the plastic flow appears. The peak effect occurs when one enters the plastic regime and the lattice tearing first enhances the critical current density j_c and then suppresses it. ''Steps'' in the curve of velocity-force dependence and its differential are also found in the plastic regime. For the finite-temperature case, we see evidence of plastic and filamentary flow at low driving forces and temperatures. At high driving forces and low enough temperatures, evidence of an ordering of the moving vortices is seen in the flux flow regime. Our results are in agreement with all the previous simulations and recent experiments.

I. INTRODUCTION

Recently much attention has been focused on the driven disordered vortex lattice, due to its direct relevance to typical transport measurements. It has been established that[1,2] for all but very weak pinning, the vortex lattice is plastically deformed and the onset of vortex motion takes place through channels. This result goes beyond the applicability of the collective pinning theory for *IV* characteristics.[3] Shi and Berlinsky[4] proposed that even in the case of arbitrary weak random potential, there are regions of the vortex lattice where the strain on the vortex lattice is large enough that ''phase slips'' occur in the vortex lattice, and the motion is unstable to plastic flow in the form of channels. Thus the topological nature and the consistency of the elastic description of the vortex lattice has become a subject of extensive debate.

On the other hand, the competition between vortex-vortex and vortex-pinning interactions results in a surprising and long studied phenomenon known as the ''peak effect'' (the critical current density j_c exhibits a peak as a function of field or temperature just before it vanishes). Within the framework of collective pinning theory, Pippard[5] attributed it to the softening of the shear modulus of vortex lattice and the easy compliance of the vortex lattice to the pinning configuration, which increases j_c. One difficulty with collective pinning theory is that the tearing of lattice is ignored in estimated j_c, i.e., the lattice depins elastically, not plastically. Recently Cha and Fertig[6] proposed that peak effect is associated with a transition from elastic to plastic depinning. But there is disagreement as to whether j_c is enhanced[7] or suppressed[8] by the onset of plastic motion. In principle this debate could be settled by direct imaging of the vortices near the depinning critical current. However, in the peak effect regime such experiments are exceedingly difficult because the order parameter is suppressed near the critical temperature or critical magnetic field.

Experimenters and theorists are trying to develop tools that are sensitive to the driven motion of vortices, as well as to their equilibrium configurations. In a theoretical work in the specific content of charge density wave (CDW) systems, Fisher[9] focused on the nonlinear dynamics above the onset of motion. He proposed, in analogy with static critical phenomenon, that a scaling behavior between force and velocity is expected for the onset of motion,

$$V \sim (F - F_c)^{\zeta}, \tag{1}$$

where F_c is the critical driving force and ζ is the critical exponent. Experimentally Bhattacharya and Higgins[10] found, in the layered superconductor 2H-$NbSe_2$, that the scaling fit is valid in the elastic regime for a relatively stiff vortex lattice, and that the critical exponent is the same as measured for the CDW systems.

Recent experiment[11] on a detwinned $YBa_2Cu_3O_{7-\delta}$ single crystal just below the melting transition temperature revealed a regime between pinning and plastic regimes with ''steps'' in the *IV* curve. Furthermore, an experiment[12] on the amorphous $Mo_{77}Ge_{23}$ thin films found a novel dynamical regime at low enough temperature: the onset of voltage shows abrupt steps in the differential resistance.

An actual dynamic phase transition between the plastically deformed phase and a moving lattice for the vortex lines was first proposed and numerically demonstrated in the two-dimensional (2D) system of pancake vortices by Koshelev and Vinokur.[13] Their idea is that the random pinning noise diminishes with increasing vortex velocity, allowing a high-velocity reordering.

Numerical simulations offer a unique window through which one may view the qualitative behavior of the vortices. In this work we present a numerical investigation of the dynamics of the 2D vortex system. The model is described as one of long-range interacting point vortices subject to the randomly distributed pointlike pinning centers in a thin superconducting film. The subject is the evolution in velocity-force dependence (VFD) and its differential, corresponding to the *IV* characteristics and the differential resistance dV/dI of a type-II superconductor in the mixed state, respectively.

II. MODEL

The dynamic behavior of vortex system is described by the Langevin equation

$$\eta \frac{d\mathbf{R}_i}{dt} = -\sum_{i \neq j} \nabla_i U_v(\mathbf{R}_i - \mathbf{R}_j) - \sum_{j'} \nabla_i U_p(\mathbf{R}_i - \mathbf{r}_{j'}) + \mathbf{F}_i^L(t) + \mathbf{F}_{\mathrm{dr}}, \tag{2}$$

with $\mathbf{R}_{i,j}$ and $\mathbf{r}_{j'}$ the vortex and pin coordinates. $U_v(\mathbf{R})$, $U_p(\mathbf{R}-\mathbf{r})$, $\mathbf{F}_{\mathrm{dr}}$, and η are the vortex-vortex interaction potential, the vortex-pin interaction potential, the external driving force, and the viscosity coefficient, respectively. The Langevin force $\mathbf{F}_i^L(t)$ describes the coupling with a heat bath, and can be expressed by the correlation function[14,15]

$$\langle F_{i\alpha}^L(t) F_{j\beta}^L(t') \rangle = 2\eta T \delta_{ij} \delta_{\alpha\beta} \delta(t-t'). \tag{3}$$

The vortex-vortex interaction potential is chosen as the long-range logarithmic

$$U_v(\mathbf{R}) = A_v \left(\frac{R^2}{R_v^2 - 1} \right) \ln\left(\frac{R}{R_v} \right). \tag{4}$$

The vortex-pin interaction is modeled by a conventional attracting Gaussian potential.[15,16] The parameters η is fixed to unity. All the lengths will be measured with respect to the lattice constant a_0 of the ideal triangular lattice, which is related to the vortex density n_v by $(\sqrt{3}/2)a_0^2 = n_v^{-1}$, and the scale for temperature is chosen as the ''bare'' Kosterlitz-Thouless melting temperature $T_{m0} = c_{66} a_0^2 / 4\pi$ with c_{66} the 2D shear modulus.[17] R_v and the size of pinning centers r_p are chosen to be $R_v = 2.8a_0$ and $r_p = 0.1a_0$, respectively, compared with Ref. 16. We initially place 100 vortices in a perfect triangular lattice subject to periodic triangular boundary conditions, then slowly increase the driving force F_{dr} along the horizontal symmetry axis (x axis) and measure average velocity $V_x = (1/N_v) \Sigma_{i=1}^{N_v} \mathbf{V}_i \cdot \hat{\mathbf{x}}$ and its differential dV_x/dF_x. Each time F_{dr} is increased by 0.04, then we halt the increase in F_{dr}, checking that the velocity signal V_x is stationary over time, and then collecting detailed velocity information for a long time interval, 2×10^5 molecular dynamics steps, at a single driving force.

III. RESULTS AND DISCUSSIONS

A. Zero-temperature case

In order to investigate systematically the influence of density of pinning centers to the VFD, we fix the dimensionless prefactor A_v of the vortex-vortex interaction term by $A_v = 0.01$ and vary the number of pinning centers N_p from 5 to 500. Results are plotted on a double-logarithmic scale in Fig. 1. One can see that, for small enough values of N_p (see the curves of $N_p = 5$ and $N_p = 10$), only elastic deformations of the lattice occur and the VFD response is basically linear. With larger value of N_p (see the curve of $N_p = 20$), there exists a critical driving force F_c ($F_c \approx 0.16$ for $N_p = 20$), below which the lattice is pinned. In the pinning regime the velocity is generated mainly by rearrangements of topological defects, producing a very slow and unsteady advance of the pinned lattice which is a characteristic feature of the pinned elastic medium driven by a driving force.[18] This advance reduces with increasing the value of N_p (comparing the curve of $N_p = 20$ with the curve of $N_p = 40$, one can see this point). When N_p is larger than certain value ($N_p \approx 50$), the small advance of pinned lattice disappears below F_c and the vortices start to become permanently trapped, consistent with the results for dense distribution of pinning centers by Faleski, Marchetti, and Middleton,[19] where the interaction between vortices was described as a short-range model. F_c increases with increasing the value of N_p. This is in agreement with the simulation results,[18] in which a Gaussian-like form for the vortex-vortex interaction potential was chosen and a molecular-dynamics-annealing method was used. Further increasing the driving force, the pinning force becomes small relative to the driving force and all the vortices tend to move with the same velocity, approaching the asymptotic value $V_x = F_x$ and independent on the density of pinning centers.[20]

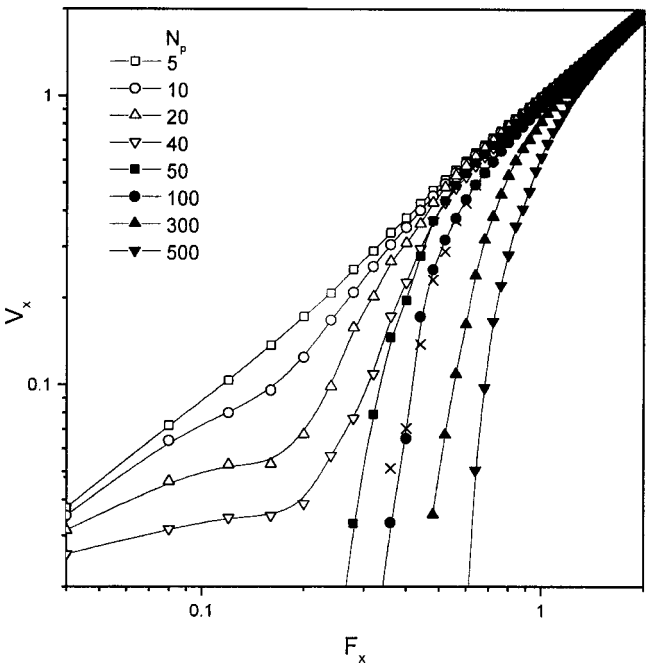

FIG. 1. Series of VFD curves for different numbers of pinning centers (assuming $A_v = 0.01$). Crosses for $N_v = 50$ ($N_p = 50$) are shown to display the finite-size effects.

The most prominent behavior is that the velocity rises concave upwards from F_c below certain value of N_p ($N_p \sim 50$), above which convex upwards occurs. The concave and convex features are the typical depinning characteristics of the elastic and plastic media, respectively.[10] In the elastic regime different vortices are bundled together, forming different Larkin domains, and only large enough driving forces can drive vortices within the same domain to depin coherently. Therefore the velocity rises concave upwards from F_c. On the contrary, because different vortices are trapped in different channels in the plastic regime, the onset of motion for the defective vortex lattice is qualitatively different from that in the elastic regime. Small driving forces can cause different vortices to depin independently, and the velocity rises rapidly and convex upwards from F_c.

In detail, we give the quantitative consideration in the following. It is known[14] that elastic collective pinning is expected when the inequality

TABLE I. The calculated results of $W^{1/2}/c_{66}$ for different values of N_p, assuming $A_v=0.01$.

N_p	5	10	20	40	50	100	300	500
$W^{1/2}/c_{66}$	0.06	0.11	0.12	0.46	0.57	1.15	3.44	5.74

$$W^{1/2}/c_{66} \ll 1 \tag{5}$$

holds, where

$$W = n_v^2 \frac{N_p}{N_v} \int d^2\mathbf{r} (\nabla U_p)^2 = \frac{\pi N_p}{4N_v} n_v^2 r_p^2 \tag{6}$$

is the mean square value of the random pinning force, and the nature of pinning depends on the relation between the 2D shear modulus c_{66},

$$c_{66} = 0.79 n_v A_v . \tag{7}$$

The calculated results of $W^{1/2}/c_{66}$ for different values of N_p are listed in Table I. One can see that, for the dilute distribution of pinning centers, the pinning is weak and can be described by the collective pinning theory; for the dense distribution of pinning centers, the pinning becomes strong, falling outside the region of validity of the collective theory. The results are in agreement with the above discussion.

To investigate the dependence of our results upon the system size, we vary the system to a smaller one. For one of $N_v=50$ vortices with $N_p=50$ randomly distributed pointlike centers (keep $N_p/N_v=\frac{50}{50}=\frac{100}{100}$ fixed), the results are shown in the Fig. 1 by crosses. Comparing with the curve of $N_v=100$ ($N_p=100$), we find that the finite-size effects are so small that can be neglected.

Using the monotonic relationship between the shear modulus c_{66} and the dimensionless prefactor A_v of the vortex-vortex interaction term,[14,15] we model vortex lattices with varying degrees of softness by changing A_v over 4 orders of magnitude from $A_v=3$ to $A_v=0.0001$ (N_p is fixed by $N_p=200$), in contrast to previous simulations,[21,22] where only the extremely soft vortex lattices have been considered. We find remarkable changes in the gross features of VFD curves as A_v is varied. Simulation results are presented in Fig. 2. From Fig. 2 one can see that there exists a critical driving force F_c in each curve of VFD, below which the lattice is pinned and the velocity is generated mainly by rearrangements of topological defects, producing a so small advance of the pinned lattice that can be neglected. F_c increases with A_v decreasing, consistent with recent simulation results[23] where a modified Bessel function form for the vortex-vortex interactions was chosen. For stiff vortex lattice with large value of A_v, the curve of VFD is linear down to F_c. The scaling fit can be obtained above F_c. This is a general feature of elastic medium. For $A_v=3$ the apparent critical exponent $\zeta=1.11\pm0.05$, as shown in the inset of Fig. 2. This is close to the measured for the CDW systems,[24] and is in agreement with the experiment on layered superconductor 2H-$NbSe_2$.[10] The apparent critical exponent measures the collective motion of the vortex lattice which is uniform on average.[10] We thus attribute this regime to the coherent motion of an elastic vortex lattice, and the lattice depins elastically. The depinning can be well described by the collective pinning theory, and has been discussed in Refs. 14–16. For soft vortex lattices with small values of A_v, plastic flow occurs, producing a pronounced upward curvature induced by defects in the vortex lattice. Crossover to the plastic regime is accompanied by the change in the shape of VFD. The scaling fit cannot be obtained in this case. A prominent feature is, as one enters the plastic regime, that steps appear between the pinned and plastic region in the curve of VFD. This is due to the coexistence of pinned vortices and moving ones, i.e., the flow is filamentary. At a moment, the only effect of increasing F_x is to increase the speed of the vortices inside the channel, while the structure of the channel and pinned vortices remains stable in a wide region of F_x. When increasing F_x, at another moment, the channel becomes unstable and the system switches to a different attractor characterized by a new spatial channel structure, which again stable in a range of F_x. This results in sudden jumps in the VFD curve between different linear regimes,[25] consistent with the recent experiments on amorphous $Mo_{77}Ge_{23}$ (Ref. 12) and $YBa_2Cu_3O_{7-\delta}$.[11]

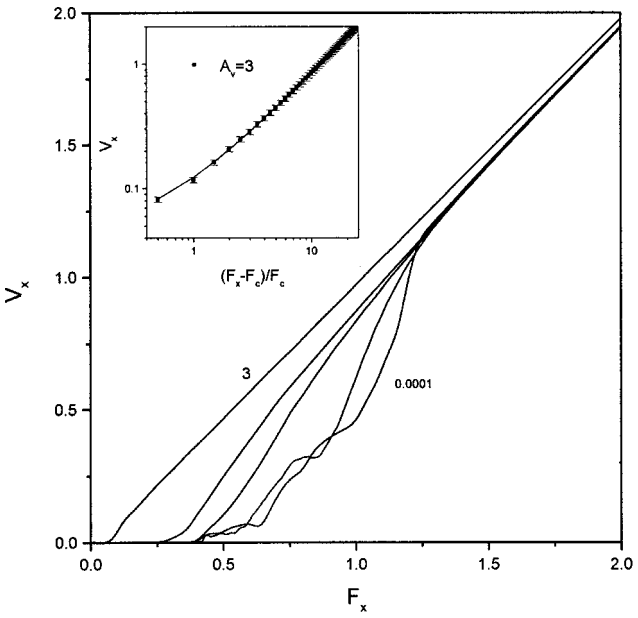

FIG. 2. Series of VFD curves for different values of A_v (from left to right) $=3$, 0.1, 0.01, 0.001, 0.0001, assuming $N_p=200$. Inset: Scaling behavior in the elastic regime; the line marks the apparent critical exponent $\zeta=1.11$.

Another obvious behavior in Fig. 2 is a dramatic change in the VFD curve with a pronounced inflection point when one enters the plastic regime, i.e., change of curvature. As the value of A_v is decreased, the inflection point moves to large value of the driving force. The systematics of evolution of these curves with decreasing the value of A_v is better illustrated by the differential curve dV_x/dF_x (proportional to the differential resistance, $R_d=dV/dI$) in Fig. 3. One can notice that dV_x/dF_x shows a peak slightly above F_c, and the position of peak moves to the large driving force. The peak value exceeds the normal value and thus does not represent R_f, the asymptotic flux flow value. In the elastic regime only a small peak in dV_x/dF_x appears, and crossing over the peak, dV_x/dF_x decreases rapidly and monotonically to the asymptotic flux flow value. When one enters the plastic regime, there is a large peak in dV_x/dF_x which increases with decreasing the value of A_v. Crossing over the peak,

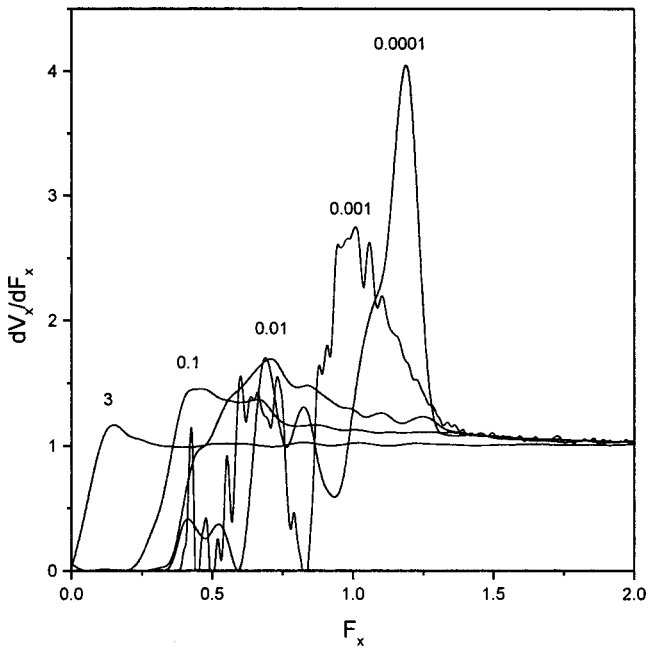

FIG. 3. Evolution of the differential curve dV_x/dF_x with decreasing the value of A_v (from left to right) $=3$, 0.1, 0.01, 0.001, 0.0001.

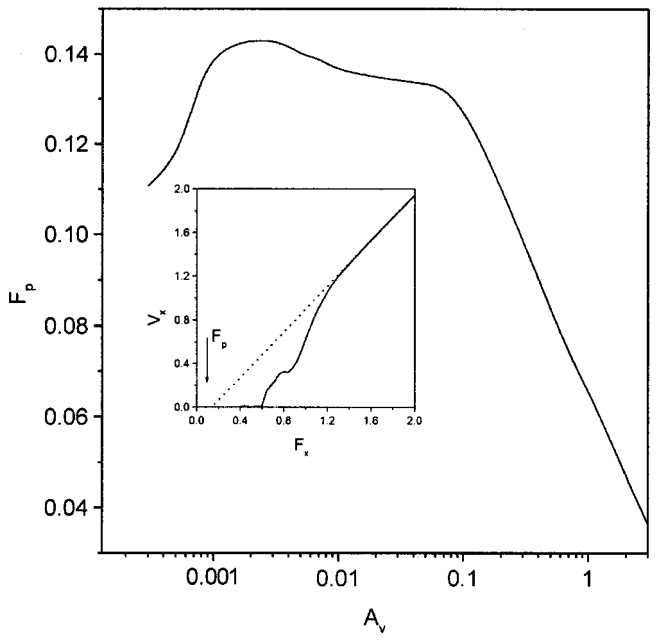

FIG. 4. Average pinning force F_p vs A_v. Inset: extrapolation from the flux flow regime to obtain the pinning force F_p.

dV_x/dF_x decreases with large numbers of ''fingerprints'' to the asymptotic flux flow value, consistent with the recent experiment[26] where the authors attributed the ''fingerprint'' phenomenon to the crossover from the weak to strong disorder. The fact that no fingerprint appears for soft enough vortex lattice in the Fig. 3 (see the curve of $A_v=0.0001$) strongly supports this viewpoint.

We reexamine the VFD curves in the Fig. 2. At high driving forces, the VFD curves all exhibit a well-defined linear region of flux flow. If we extrapolate this linear $V_x=(F_x-F_p)R_{ff}$ back to the F_x axis, as illustrated in the inset of Fig. 4. The intercept in F_x axis gives us the average pinning force F_p (proportional to the critical current density j_c) that the vortices feel in the flux flow regime. From Fig. 4 one can find that peak effect occurs when one enters the plastic regime, and the lattice tearing first enhances F_p then suppresses F_p. It is believed that[6] plastic flow, when it first sets in with decreasing c_{66}, is associated with an increase in critical current j_c; for low enough values of c_{66}, river flow motion sets in, and F_p becomes proportional to c_{66}. We agree with this viewpoint.

B. Non-zero-temperature case

We change the temperature over 4 orders from high to very low (fix N_p and A_v by $N_p=400$ and $A_v=0.001$, respectively). Different VFD curves from high to low temperatures are plotted on a double-logarithmic scale in Fig. 5. The results at low temperatures (see the curve of $T/T_{m0}=0.1$) clearly show that there are three distinct regimes. (i) At low driving forces ($F_x<0.36$), the lattice is pinned and the velocity is generated mainly by rearrangements of topological defects, which produce a very slow and unsteady advance of the pinned lattice. (ii) At moderate F_x ($0.52<F_x<1.0$), the VFD curve is strongly nonlinear. (iii) At high F_x, the linear VFD respondence restores. These are in qualitative agreement with the previous simulation results.[21] In addition, steps occur just above the depinning below certain temperature. ''Steps'' behavior can be seen most clearly in the curves of $T/T_{m0}=0.5$ and $T/T_{m0}=1$. With increasing the temperature, the influence of disorder decreases, leading to a decrease of the critical pinning force F_c and the restoration of the linear VFD at small forces. These can be explained as follows[27] that the thermal fluctuations of the individual vortex lines leads to a dynamical sampling and hence averaging of the disorder potential over the spatial extent of the thermal displacement $\langle u^2\rangle_{\rm th}^{1/2}$. Thermal disorder hence opposes

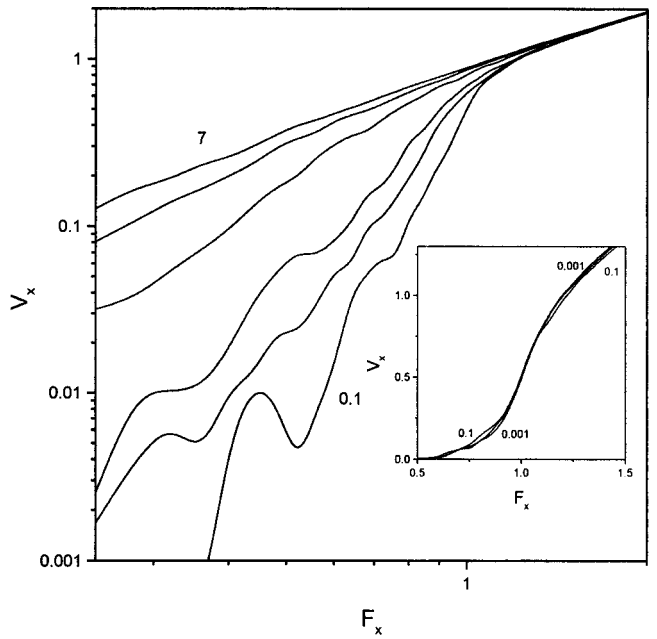

FIG. 5. Series of VFD curves at T/T_{m0} (from top to bottom) $=7$, 5, 3, 1, 0.5, 0.1, assuming $N_p=400$ and $A_v=0.001$. Inset: Three VFD curves at very low temperatures $T/T_{m0}=0.1$, 0.01, 0.001.

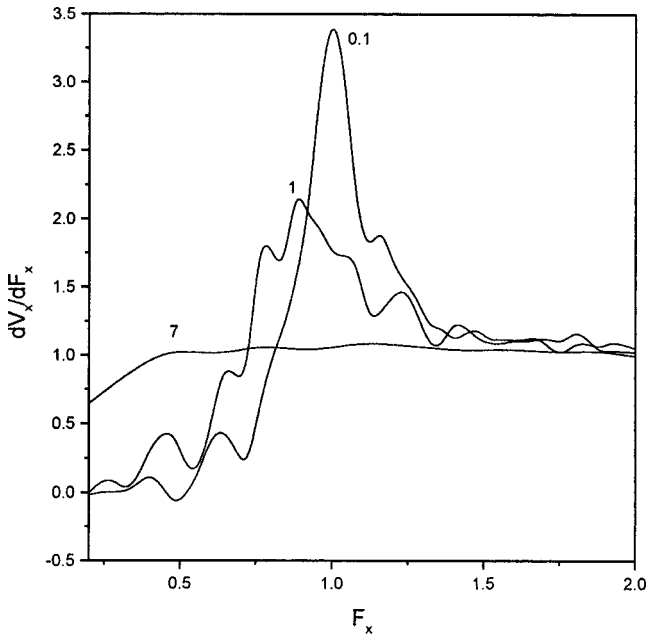

FIG. 6. dV_x/dF_x vs F_x at T/T_{m0} (from left to right) $=7$, 1, 0.1.

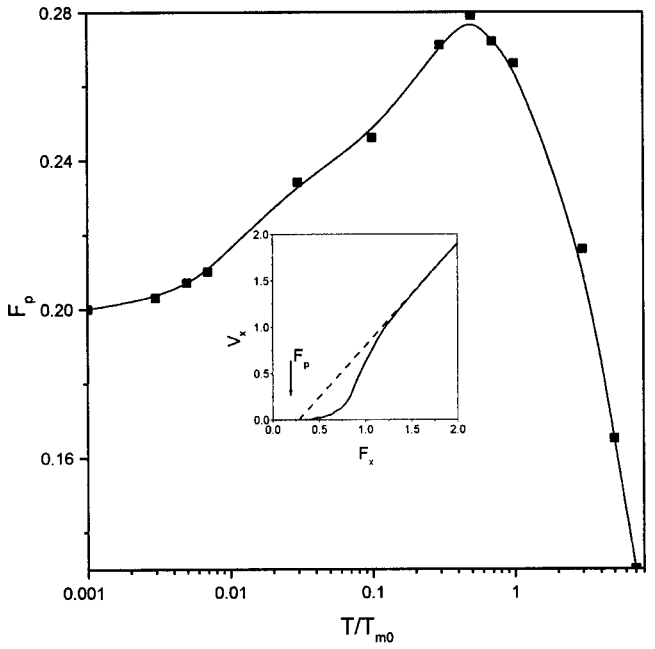

FIG. 7. Average pinning force at high driving force vs temperature. Inset: The extrapolation from the flux flow regime to obtain the average pinning force.

quenched disorder via a smoothing of the disorder potential and thereby reduces the critical pinning force in the system. At high temperatures, the interaction between vortices becomes of importance. Therefore when the temperature becomes high enough, the linear behavior of VFD is restored even at small forces.

To see clearly the above features, we present three differential curves of VFD at $T/T_{m0}=7$, 1, 0.1 in Fig. 6. One can see that there is no peak in the high temperature curves, and dV_x/dF_x vs F_x curve rises monotonically with increasing F_x and asymptotically approaches the flux flow value. The corresponding VFD curve in the Fig. 5 also exhibits a smooth monotonic rise and asymptotic approach to its linear flux flow behavior. This corresponds to the classical flux flow picture.[14] The behavior of the low-temperature curve is different. A peak appears in the dV_x/dF_x vs F_x curve, which exceeds the flux flow value. The peak arises since dV_x/dF_x at first increases as a driving force is applied and the vortices depin and flow defectively, and then drops as the vortices order and the dynamic friction they experience decreases. The peak in dV_x/dF_x vs F_x curve is associated with a drop in the defect density of the moving vortex configuration, and becomes more pronounced in the curves measured at lower temperatures. ''Fingerprints'' are also observed crossing over the peak in the low-temperature curves, as found in the recent experiment on amorphous $Mo_{77}Ge_{23}$.[12] An interesting behavior is that there are most numbers of steps in the moderately low-temperature curves. When the temperature is further decreased, the number of steps shrinks. It suggests some increase in the order of the system of vortices at the very low temperature.

The ordering at very low temperatures can be seen explicitly in the inset of Fig. 5, where we present three VFD curves at very low temperatures $T/T_{m0}=0.1$, 0.01, 0.001. One can see that a pronounced kink appears in the VFD curves, which signifies a range of the driving force over which the differential exceeds the flux flow value.

To further characterize this ordering, we reexamine the VFD curves shown in Fig. 5. At high driving force, VFD curves all also exhibit a well-defined linear region of flux flow. As the above, we extrapolate this linear $V_x=(F_x-F_p)R_{ff}$ back to the driving force axis, as illustrated in the inset of Fig. 7. The fact that F_p decreases as the temperature drops below T^* ($T^*\approx 0.5T_{m0}$) suggests that the rigidity of moving vortex system increases as the temperature is lowered below T^*. The pinning in these films at low temperature has previously been shown to be collective,[28] so the theory of Larkin and Ovchinnikov can give us a qualitative idea of the origin of this increase in the rigidity of the moving vortex configuration. In this theory, the transverse correlation length is given by $R_c \propto \sqrt{1/I_c}$, where I_c is the critical current and proportional to the average pinning force F_p. Hence, the drop in F_p at low temperatures implies an increase in the correlation area in the flux flow regime.

The drop in F_p, the pronounced peaks in the dV_x/dF_x vs F_x curves and shrinking of the steps in the curves of VFD as well as its differential are all observed at temperature below T^*, consistent with recent simulations and experiment. These features suggest an ordering of the system at high driving force in this temperature range. The peak in the differential curve characterizes the driving force at which the ordering occurs for a given temperature. The decreasing F_p indicates an increasing order in the moving vortex configuration (in the high driving force limit beyond the peak) as the temperature is lowered below T^*.

In summary, we have numerically investigated the dynamics of driven vortex lattice subject to the randomly distributed pointlike pinning centers in a thin superconducting film. At zero temperature, crossover from elastic to plastic depinnings was observed with increasing the density of pinning centers. With the lattice softness, the scaling fit between force and velocity obtained in the elastic regime becomes invalid when the plastic flow appears. A peak effect occurs

when one enters the plastic regime, and the lattice tearing first enhances the critical current density j_c then suppresses it. ''Steps'' in the curve of velocity-force dependence and its differential have also been found in the plastic regime. For the finite-temperature case, we found the evidence of plastic and filamentary flow at low driving forces and temperatures; at high driving forces and low enough temperatures, evidence of an ordering of the moving vortices was seen in the flux flow regime. Our results were in agreement with all the previous simulations and recent experiments.

ACKNOWLEDGMENTS

This work was supported by the National Center for Research and Development on Superconductivity of China. Cao and Ying acknowledge the support of NNSC of China under Grant No. 19975041.

[1] E. H. Brandt, Phys. Rev. Lett. **50**, 1599 (1983).
[2] H. J. Jensen, Y. Brechet, and A. Brass, J. Low Temp. Phys. **74**, 293 (1989).
[3] A. I. Larkin and Yu. N. Ovchinnikov, J. Low Temp. Phys. **34**, 409 (1979).
[4] An-Chang Shi and A. J. Berlinsky, Phys. Rev. Lett. **67**, 1926 (1991).
[5] A. B. Pippard, Philos. Mag. **19**, 217 (1969).
[6] Min-Chui Cha and H. A. Fertig, Phys. Rev. Lett. **80**, 3851 (1998).
[7] A. I. Larkin, M. C. Marchetti, and V. M. Vinokur, Phys. Rev. Lett. **75**, 2992 (1995); M. J. Higgins and S. Bhattacharya, Physica C **257**, 232 (1996).
[8] H. Pastoriza and P. H. Kes, Phys. Rev. Lett. **75**, 3525 (1995); W. K. Kwok, J. A. Fedrich, V. M. Vinokur, A. E. Koshelev, and G. W. Crabtree, *ibid.* **76**, 4596 (1996).
[9] See D. S. Fisher, in *Nonlinearity in Condensed Matter*, edited by A. R. Bishop *et al.* (Springer Verlag, New York, 1987).
[10] S. Bhattacharya and M. J. Higgins, Phys. Rev. Lett. **70**, 2617 (1993).
[11] G. D'Anna, P. L. Gammel, H. Safar, G. B. Alers, and D. J. Bishop, Phys. Rev. Lett. **75**, 3521 (1995).
[12] M. C. Hellerqvist, D. Ephron, W. R. White, M. R. Beasley, and A. Kapitulnik, Phys. Rev. Lett. **76**, 4022 (1996).
[13] A. E. Koshelev and V. M. Vinokur, Phys. Rev. Lett. **73**, 3580 (1994).
[14] A. E. Koshelev, Physica C **198**, 371 (1992).
[15] Yigang Cao and Zhengkuan Jiao, Physica C **321**, 177 (1999).
[16] E. H. Brandt, J. Low Temp. Phys. **53**, 71 (1983).
[17] D. S. Fisher, Phys. Rev. B **22**, 1190 (1980).
[18] A. Brass, H. J. Jensen, and A. J. Berlinsky, Phys. Rev. B **39**, 102 (1989).
[19] M. C. Faleski, M. C. Marchetti, and A. A. Middleton, Phys. Rev. B **54**, 12 427 (1996).
[20] K. Moon, R. T. Scalettar, and G. T. Zimani, Phys. Rev. Lett. **77**, 2778 (1996).
[21] S. Ryu, M. Hellerqvist, S. Doniach, A. Kapitulnik, and D. Stroud, Phys. Rev. Lett. **77**, 5114 (1996).
[22] C. Reichhardt, C. J. Olson, and F. Nori, Phys. Rev. Lett. **78**, 2648 (1997).
[23] C. J. Olson, C. Reichhardt, and F. Nori, Phys. Rev. Lett. **81**, 3757 (1998).
[24] S. Bhattacharya, M. J. Higgins, and J. P. Stokes, Phys. Rev. Lett. **63**, 1503 (1989).
[25] N. G. Jensen, A. R. Bishop, and D. Dominguez, Phys. Rev. Lett. **76**, 2985 (1996).
[26] S. Bhattacharya and M. J. Higgins, Phys. Rev. B **52**, 64 (1995).
[27] G. Blatter, M. V. Feigel'man, V. B. Geshkenbein, A. I. Larkin, and V. M. Vinokur, Rev. Mod. Phys. **66**, 1125 (1994).
[28] W. R. White, A. Kapitulnik, and M. R. Beasley, Phys. Rev. Lett. **70**, 670 (1993).